

Halogenated Metalloporphyrin Complexes as Catalysts for Selective Reactions of Acyclic Alkanes with Molecular Oxygen

James E. Lyons, Paul E. Ellis, Jr., and Harry K. Myers, Jr.

Research and Development Department, Sun Company, Inc., Marcus Hook, Pennsylvania 19061-0835

Received November 29, 1994; revised February 22, 1995

We have shown that halogenation of the porphyrin ring of a metalloporphyrin complex can convert a catalytically inactive material into an exceptionally active catalyst for the selective reaction of an alkane with molecular oxygen. The greater the degree of halogenation of the ring, the greater is the catalytic activity of the metal complex. The product profile, while characteristic of radical reactions, is sensitive to the nature of the metal center. Iron complexes are generally more active than those of cobalt, manganese, or chromium. The activity of iron complexes is directly related to the Fe(III)/(II) reduction potential of the porphyrin complex. There is also a similar correlation between the Fe(III)/Fe(II) reduction potential and the rate at which iron haloporphyrin complexes decompose alkyl hydroperoxides. *These iron perhaloporphyrin complexes are not only the most active known liquid phase alkane air-oxidation catalysts, they are also the most active hydroperoxide decomposition catalysts known to date.* The nature of the products formed is dependent on the structure of the aliphatic substrate that is oxidized and can be rationalized by a catalytic pathway that very efficiently generates alkyl and alkoxy radicals at low temperatures. The relationship between the electrochemical properties of these complexes and the rates of alkane oxidation and hydroperoxide decomposition lends insight into possible mechanisms of catalytic activity. © 1995 Academic Press, Inc.

INTRODUCTION

The selective reaction of an alkane with molecular oxygen to give an alcohol or carbonyl compound without extensive oxidative cleavage or concomitant combustion has considerable potential as an inexpensive means of producing valuable oxygenates. Selective oxidation of an alkane is usually hard to achieve thermally since under conditions necessary to promote facile autooxidation, alkane oxidations are often difficult to stop short of combustion (1). Metalloporphyrin complexes have long been known to catalyze the oxidative hydroxylation of alkanes in a biomimetic manner, but these complexes have required either (a) stoichiometric oxygen atom donors other than oxygen (2–10), (b) sacrificial coreductants (11–20), (c) electrochemical reduction (21, 22), or (d) photolytic assistance (23, 24).

Recent work by the authors (25–34) and others (35–38) has shown that halogenated metalloporphyrins are efficient catalysts for the direct reaction of alkanes with oxygen to give alcohols and/or carbonyl compounds at unprecedented rates under very mild conditions. No coreductants or stoichiometric oxidants are required (25–38). Neither is it necessary to employ photochemical or electrochemical techniques in these oxidations. Because of the potential utility of a direct catalytic reaction of an alkane with molecular oxygen in a selective manner, we report the results of a study on the oxidation of a series of acyclic alkanes under mild conditions catalyzed by halogenated metalloporphyrins.

RESULTS AND DISCUSSION

Oxidations of Isobutane and Propane

We have found that chromium, manganese, and iron complexes of halogenated porphyrinato ligand systems (Fig. 1) are active catalysts for the oxidation of unactivated acyclic alkanes having either secondary or tertiary carbon–hydrogen bonds. Primary C–H bonds are quite resistant to oxidative attack in the presence of these catalysts. Table 1 shows the results of oxidations of isobutane at 80°C in benzene solutions of metalloporphyrin complexes using molecular oxygen as the oxidant. *tert*-Butyl alcohol is the predominant product of the reaction, being formed in yields of about 90%. Several points are evident from the data presented in Table 1. First, halogenation of the phenyl groups of tetraphenylporphyrinatometal complexes causes a large increase in their catalytic activity. Second, halogenation of the *meso*-phenyl groups on the macrocycle has a greater effect on the catalytic activity of iron complexes than on those of manganese and chromium. The effect on catalytic oxidation activity of *meso*-phenyl halogenation of metallotetraphenylporphyrin complexes is in the order Fe > Mn > Cr. Thus, iron haloporphyrin complexes are the most active of those complexes that we have examined. The catalytic oxidation of isobutane using tetrakis(pentafluorophenyl)porphyrin

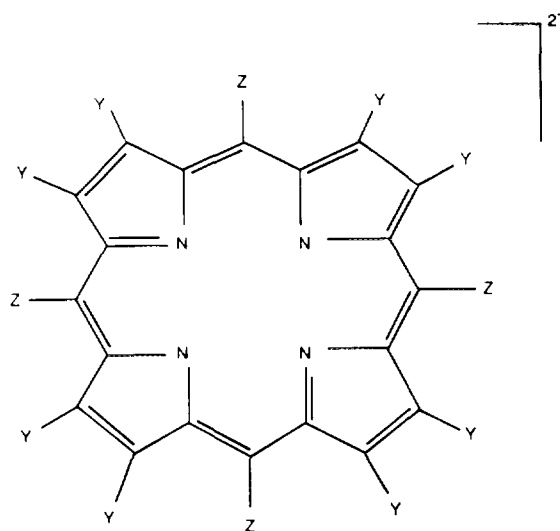


FIG. 1. The substituted porphyrinatoligand; Y = β -Cl, Br, or H; Z = C_6H_5 (TPP), o - $C_6H_4Cl_2$ (TPP Cl_2), or C_6F_5 (TPPF $_{20}$).

rinatoiron hydroxo, azido, and chloro complexes is shown in Fig. 2. Rates are rapid and no induction periods are apparent. Table 2 shows the effect of the degree of halogenation on the catalytic oxidation activity of porphyrinatoiron chloro, azido, oxo, and hydroxo complexes. The isobutane conversion levels after 6 h at 80°C are substantial, reaching as high as 45% when Fe(TPPF $_{20}\beta$ -Br $_8$)Cl I is used as the catalyst. Figure 2 indicates the relative catalytic activities of the hydroxo, azido, and chloro forms of Fe(TPPF $_{20}$)X. It is interesting to note that any induction period, if one exists, must be very short.

Table 3 shows the results of oxidations of isobutane at 60°C in the presence of perhaloporphyrinatometal azide complexes. After 6 h at 60°C in the presence of Fe(TPPF $_{20}\beta$ -Cl $_8$)N $_3$, *tert*-butyl alcohol was formed to 90% selectivity at an isobutane conversion of 27%. At 80°C (Table 1), complexes having axial chloride provide suitable catalysts, whereas for high activity at 60°C or lower it is desirable to use the azido or hydroxo forms of the catalyst. Combining the results in Tables 1, 2, and 3, it can be seen that the greater the extent of halogenation of the porphyrin macrocycle, the more active is the metal complex for alkane oxidation. Table 4 shows the results of oxidations of propane at 125°C in the presence of perhaloporphyrinatometal azide complexes. Although higher

^I Abbreviations used: TPP, *meso*-tetraphenylporphyrin dianion; TPP β -Br $_4$, *meso*-tetraphenyl β -tetrabromoporphyrin dianion; TPPCl $_8$, *meso*-tetrakis(2,6-dichlorophenyl)porphyrin dianion; TPPCl $_8\beta$ -Br $_4$, *meso*-tetrakis(2,6-dichlorophenyl) β -tetrabromoporphyrin dianion; TPPF $_{20}$, *meso*-tetrakis(pentafluorophenyl)porphyrin dianion; TPPF $_{20}\beta$ -Cl $_8$, *meso*-tetrakis(pentafluorophenyl)- β -octachloroporphyrin dianion; and TPPF $_{20}\beta$ -Br $_8$, *meso*-tetrakis(pentafluorophenyl)- β -octabromoporphyrin dianion.

TABLE 1

Effect of Fluorination of the *meso*-Phenyl Groups on the Activity of Tetraphenylporphyrinatometal Complexes for Reactions of Isobutane with Oxygen^a

Catalyst	Catalyst (mmol)	Catalyst turnovers ^b	Selectivity to <i>tert</i> -butyl alcohol (%) ^c
Fe(TPP)Cl	0.025	0	—
Fe(TPPF $_{20}$)Cl	0.016	2040	90
Fe(TPP)N $_3$	0.013	130	93
Fe(TPPF $_{20}$)N $_3$	0.016	2060	89
Mn(TPP)N $_3$	0.013	180	88
Mn(TPPF $_{20}$)N $_3$	0.016	750	87
Cr(TPP)N $_3$	0.025	280	89
Cr(TPPF $_{20}$)N $_3$	0.016	450	97
[Fe(TPP)] $_2$ O	0.013	0	—
[Fe(TPPF $_{20}$)] $_2$ O	0.007	1730	92

^a Isobutane (7 g) was oxidized (6 h) in 25 ml benzene containing the designated catalyst at 80°C under 100 psig O $_2$.

^b Mol O $_2$ consumed/mol catalyst used.

^c (Mol *tert*-butyl alcohol/mol liquid product) \times 100.

temperatures are required to oxidize the secondary C-H bond of propane rather than the tertiary C-H bond of isobutane, the selectivity to a mixture of acetone and isopropyl alcohol is high and only small amounts of carbon oxides are formed. Because of the large quantity of pro-

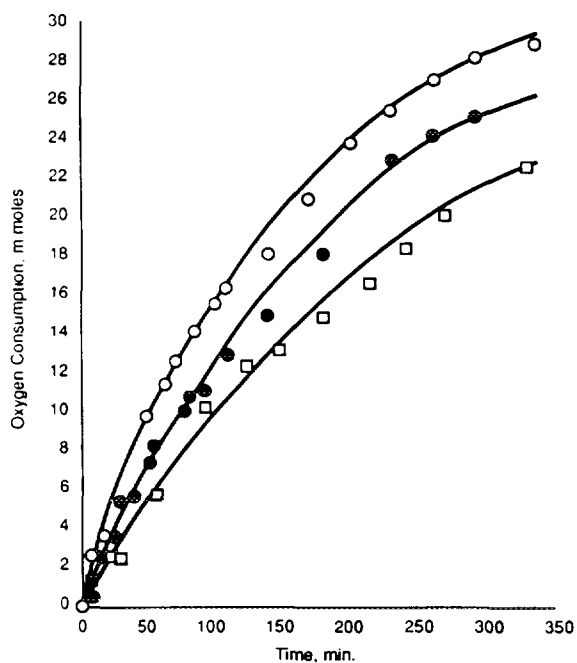


FIG. 2. Oxidation of isobutane in benzene at 80°C using Fe(TPPF $_{20}$)X; X = Cl (\square); N $_3$ (\bullet); and OH (\circ) as axial ligands.

TABLE 2

 Effect of Ring Halogenation on the Isobutane Oxidation Activity of Porphyrinatoiron(III) Complexes^a

Catalyst	Catalyst (mmol)	O ₂ Uptake (mmol)	TO ^b	Selectivity to TBA (%)
Fe(TPP)Cl	0.025	0.0	—	—
Fe(TPPβ-Br ₄)Cl	0.013	2.0	155	—
Fe(TPPCl ₈)Cl	0.019	5.0	263	89
Fe(TPPCl ₈ β-Br ₄)Cl	0.020	17.3	865	83
Fe(TPPF ₂₀)Cl	0.016	32.6	2040	90
Fe(TPPF ₂₀ β-Br ₈)Cl	0.013	40.2	3090	89
Fe(TPP)N ₃	0.013	1.7	130	89
Fe(TPPβ-Br ₄)N ₃	0.013	2.3	177	—
Fe(TPPCl ₈)N ₃	0.023	15.0	653	80
Fe(TPPCl ₈ β-Br ₄)N ₃	0.023	21.5	934	82
Fe(TPPF ₂₀)N ₃	0.016	33.0	2060	89
[Fe(TPP)] ₂ O	0.019	0.0	0	—
[Fe(TPPβ-Br ₄)] ₂ O	0.013	0.0	0	—
Fe(TPPCl ₈)OH	0.013	9.2	711	83
[Fe(TPPF ₂₀)] ₂ O	0.013	24.0	1846	84
[Fe(TPPF ₂₀)OH	0.013	29.2	2245	82

^a A solution of the catalyst in 25 ml benzene containing 7 g of isobutane was stirred at 80°C under 100 psig of O₂ for 6 h.

^b Mol O₂ consumed/mol catalyst used.

TABLE 3

 Isobutane Oxidations Catalyzed by Perhaloporphyrin Complexes^a

Catalyst	T (°C)	TO ^b	<i>t</i> -BuOH Selectivity (%)
Fe(TPPF ₂₀ β-Br ₈)N ₃	60	1550	87
	40	670	89
	27	620	na
Fe(TPPF ₂₀ β-Cl ₈)N ₃	60	1800	90
	40	760	92
Cr(TPPF ₂₀ β-Br ₈)N ₃	60	110	92
Cr(TPPF ₂₀ β-Cl ₈)N ₃	80	450	88
Mn(TPPF ₂₀ β-Br ₈)N ₃	60	270	87
Mn(TPPF ₂₀ β-Cl ₈)Cl + NaN ₃ ^c	80	1289	86
Mn(TPPF ₂₀ β-Cl ₈)Cl + NaN ₃ ^c	60	156	88
Co(TPPF ₂₀ β-Cl ₈)	60	355	91

^a Isobutane (7 g) was oxidized (6 h) in 25 ml benzene at the designated temperature under 100 psig oxygen using 0.013 mmol of the designated catalyst.

^b Mol O₂ consumed/mol catalyst used.

^c After the reaction mixture was warmed for 6 h as indicated in footnote a, the reaction mixture was cooled to room temperature, 10 mg of NaN₃ was added, and the procedure was repeated according to footnote a. The TO are calculated based on the second 6-h period.

TABLE 4

 Propane Oxidations Using First-Row Metal Complexes of TPPF₂₀β-Br₈ as Catalysts^a

Catalyst	Time (h)	T (°C)	TO ^b	IPA/acetone ^c
Fe(TPPF ₂₀)N ₃	3	125	330	0.8
Fe(TPPF ₂₀ β-Br ₈)N ₃	4.5	125	541	0.9
Cr(TPPF ₂₀)N ₃	4.5	125	41	<0.1
Cr(TPPF ₂₀ β-Br ₈)N ₃	4.5	125	87	0.6
Mn(TPPF ₂₀)N ₃	3	125	0	—
Mn(TPPF ₂₀ β-Br ₈)N ₃	4.5	125	87	1.0

^a Propane (1.36 mol) was added to benzene (48 ml) containing the catalyst (0.013 mmol). The solution was stirred for 3 h at 125°C under 1000 psig of air in a glass-lined autoclave.

^b Mol of acetone plus isopropyl alcohol formed per mol of catalyst used.

^c Molar ratio of isopropyl alcohol to acetone formed.

pane that is used, conversion is low, reaching only 0.6% after 3 h when Fe(TPPF₂₀β-Br₈)N₃ is the catalyst.

Table 5 shows the results of oxidations with conventional cobalt oxidation catalysts. Prior to our work on the perhaloporphyrin complexes, the bispyridyliminoisoindoline (BPI) complexes were among the most active alkane autooxidation catalysts known (39, 40). A comparison of the results of Table 5 with those of Tables 1, 2, 3 and 4

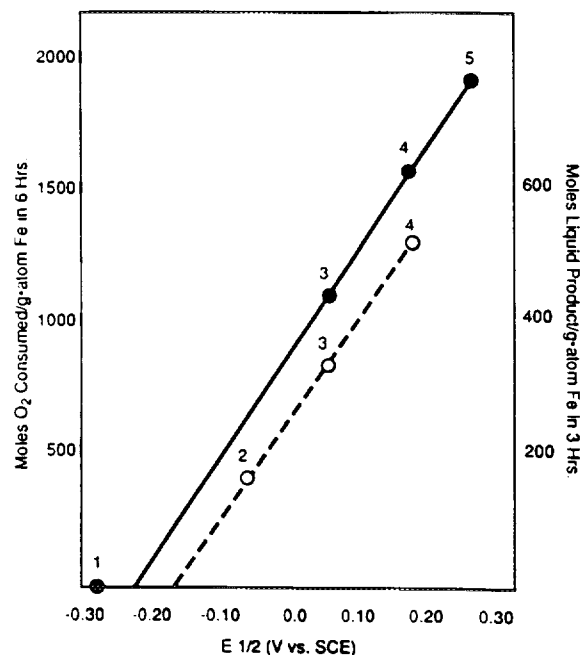


FIG. 3. Catalyst turnovers as a function of Fe(III)/Fe(II) oxidation potential. (—●—) Isobutane oxidations at 60°C; (---○---) propane oxidations at 125°C. See Tables 3 and 4 for experimental procedures. (1) Fe(TPP)OH; (2) Fe(TPPCl₈β-Br₄)OH; (3) Fe(TPPF₂₀)OH; (4) Fe(TPPF₂₀β-Br₈)OH; (5) Fe(TPPF₂₀β-Cl₈)OH.

TABLE 5
Alkane Oxidations Catalyzed by Cobalt Complexes

Complex	Complex (mmol)	Substrate	Reaction T ($^{\circ}\text{C}$)	Total P (psig)	Reaction time (h)	Catalyst turnovers	Product selectivity (%)		
							TBA-HP ^c	Acetone	IPA
Co(acac) ₂	0.100	<i>i</i> -C ₄ H ₁₀ ^a	80	100	6	52	89	10	—
Co(acac) ₃	0.100					15	88	10	—
Co(BPI)(OAc)	0.025					24	88	12	—
Co(BPI)N ₃	0.025					200	87	13	—
Co(BPI)(O ₂ Bu')	0.025					260	89	11	—
Co(acac) ₂	0.023	C ₃ H ₈ ^b	125	1000	3	21	—	62	35
Co(acac) ₂	0.023				18	122	—	62	35
Co(acac) ₃	0.023				3	27	—	64	33
(+ <i>t</i> -C ₄ H ₉ OOH)	(0.23)								
Co(BPI)(O ₂ Bu')	0.023				3	20	—	>90	<10

^a Isobutane (7 g) was oxidized as in Table 1.

^b Propane (60 g) was oxidized as in Table 4.

^c Mol% (TBA + TBHP).

indicates that perhaloporphyrin complexes are more active by greater than an order of magnitude than even the most active cobalt complexes currently available.

Effects of Electron Withdrawal from the Macrocycle

As the number of halogen substituents around the periphery of the porphyrin macrocycle increases, the ease of reducing Fe(III) in the coordination sphere increases (28–34, 38). Figure 3 demonstrates a regular relationship between catalytic turnovers for both isobutane and propane oxidations in a set time period and the Fe(III)/Fe(II) reduction potential of the catalyst used. Thus, as the degree of halogenation increases, the Fe(III)/Fe(II) reduction potential also increases and the catalytic activity im-

proves. These iron complexes are soluble enough in aliphatic hydrocarbons to allow reactions to proceed in neat alkane solutions (Table 6). When iron haloporphyrin complexes are dissolved in neat isobutane, oxidation to *tert*-butyl alcohol can be efficiently carried out under very mild conditions of temperature and pressure. These complexes smoothly catalyze isobutane oxidations at temperatures between room temperature and 100 $^{\circ}\text{C}$, and oxygen partial pressures between 1 and 5 atm. Reaction rate and catalyst life are unprecedented. We have achieved well over 20,000 turnovers (mol product(s) formed/mol catalyst used) in *tert*-butyl alcohol (TBA) production. Although catalyst decomposition is a problem at somewhat elevated temperatures (>60 $^{\circ}\text{C}$), well over 10,000 catalytic turnovers have been observed in the room-temperature

TABLE 6
Iron-Haloporphyrin-Catalyzed Isobutane Oxidation^a

Catalyst	T ($^{\circ}\text{C}$)	Time (h)	<i>i</i> -C ₄ H ₁₀ (mmol)	O ₂ (psi)	Reaction products (mmol)				Conversion <i>i</i> -C ₄ H ₁₀ (%)	Selectivity (%) <i>t</i> -BuOH ^b	TO ^c
					<i>t</i> -BuOH	Acetone	CO	CO ₂			
Fe(TPPF ₂₀)OH	80	3	1869	53	310	46	7	18	17	87	11,330
	24	143	1871	53	382	17	0	18	19	95	11,600
Fe(TPPF ₂₀ β-Cl ₈)Cl	80	3	1865	142	334	38	6	29	20	88	12,400
	21	120	1865	63	366	16	tr	na	20.5	95	12,730
Fe(TPPF ₂₀ β-Br ₈)Cl	80	3	1862	148	414	81	6	28	27	84	16,500
	80	3	1870	53	277	43	8	23	17	87	10,060
	24	71	1862	53	372	35	tr	27	22	92	12,150

^a Isobutane containing 0.03 mmol of dissolved catalyst was oxidized by an oxygen-containing gas mixture (75 atm; diluent, N₂) in the liquid phase (180 ml) for 3 h. Oxygen was added as it was consumed.

^b (Mol *t*-BuOH/mol liquid product) \times 100.

^c Mol (*t*-BuOH and acetone) produced/mol catalyst used.

oxidation of neat isobutane catalyzed by tetrakis(pentafluorophenyl β -octabromo)iron(III)hydroxide with no noticeable deferration or decay of the catalyst (by UV-VIS spectroscopy); see Table 6.

Mechanism Considerations

As one speculates how oxidations catalyzed by electron-deficient metalloporphyrins might proceed, it is instructive to consider the mechanism by which iron porphyrin systems are thought to catalyze C–H bond oxidations in biological systems, (Fig. 4) (41–48). In enzymatic pathways, electrons and protons are available to the heme system throughout the process. However, in our case, without coreductants (2–20) or photochemical or electrochemical assistance (21–24), monooxygenase activity of the type known to occur *in vivo* is not possible. Using the electrons of an oxygen-bridging iron catalyst system (Fig. 5) one could envision a catalytic *dioxygenase* pathway. Steps a, b, c, and f in this hypothetical pathway have precedence in the literature (49–51). There remains the question as to whether a hypothetical Fe(IV)oxo intermediate would be effective for C–H bond cleavage (Fig. 5d). Furthermore, there is the strong possibility that radicals formed from C–H bond homolysis, if it occurs (Fig. 5d), should be capable of diffusing into the reaction medium and initiating radical chain oxidation processes. Perhaps then, if radical escape occurs, the pathway shown in Fig. 5 ought to be considered a form of living initiator of alkyl radicals as well as a possible catalytic precursor of alcohol by rebound mechanisms (5, 16); see Fig. 5e.

The oxidation of organic compounds using metalloporphyrin complexes has been known for some time (52). Catalytic activity was generally poor, catalyst life was short, and prior to our work (25–28), no alkane oxidation

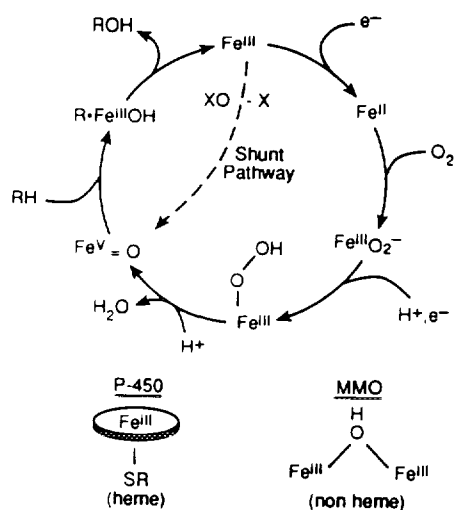


FIG. 4. Schematic representation of biological and biomimetic alkane oxidation (40–47).

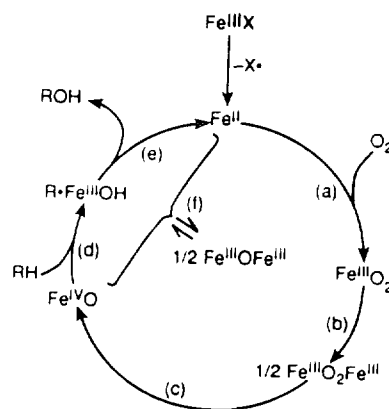


FIG. 5. Conceptual scheme for a hypothetical catalytic cycle for conversion of an alkane to an alcohol using an electron-deficient iron porphyrin complex (porphyrin ring omitted).

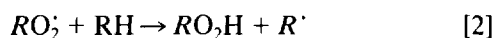
activity had been observed in unpromoted systems. Why then are the electron-deficient metalloporphyrins such good catalysts? One reason, of course, is the greater oxidative and thermal stability of the catalyst. Replacing hydrogens with halide substituents reduces the number of carbon hydrogen bonds that can undergo oxidative attack. A perhaloporphyrim complex has no carbon-hydrogen bonds which might undergo cleavage. In addition, as electron-withdrawing halo groups are introduced into the macrocyclic ring of the catalyst, the ligand itself becomes more stable to reduction by the central metal atom. It is well known that the porphyrinatoiron oxo complexes exists as the radical cation, due to electron transfer from the ligand to the iron center (35, 53). Thus, there may be a greater tendency for the active catalyst to behave as an oxo-centered radical, $(P^{\bullet})Fe=O$, than a ferryl species, $(P^+)Fe=O$, with increased electron withdrawal from the macrocycle (35).

Our work has shown that not only are electron-deficient metalloporphyrin complexes more robust, but initial rates of oxidation are much faster than those observed when nonhalogenated porphyrin complexes are used as catalysts. In fact, when halogenated metalloporphyrin catalysts are used, oxidations occur at temperatures so low that most metalloporphyrin complexes are completely inactive (Tables 1–4). Increased reaction rate can be rationalized as a result of increased Fe(III)/Fe(II) reduction potential due to electron withdrawal from the metal center by the electron-deficient ligand system. Thus, in most metalloporphyrin-catalyzed oxidations, the pool of iron exists largely or exclusively as iron(III). Initial formation of Fe(II) is disfavored, and the process represented in Fig. 5e does not occur readily. Most of the iron is rapidly converted to the μ -oxo dimer (Fig. 5f), which is usually inactive (54, 55). We have shown that μ -oxo dimers are

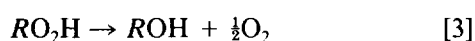
active catalysts in the perhaloporphyrin series (Tables 1 and 2) and that both iron(III) μ -oxo dimer and Fe(II) species coexist under reaction conditions (30). Therefore, although we by no means have established the existence of the scheme depicted in Fig. 5, electron-deficient porphyrins might indeed possess the necessary properties to behave in this manner, while more electron-rich porphyrin complexes do not.

Radical Routes and Hydroperoxide Intermediates

The homolysis of C–H bonds in biological systems occurs in a cage which encourages rebound to produce alcohols. Radicals do not readily escape into an aqueous medium *in vivo* as they might be expected to do, cf. Fig. 5d, when an electron-deficient metalloporphyrin catalyst is used in organic media. If a substantial amount of the reaction proceeds through a radical pathway, then a free radical inhibitor should quench the reaction. We have shown that as little as 1 mol of di-*tert*-butyl-*p*-cresol per mol of catalyst can substantially quench the oxidation reaction. Furthermore, if radical pathways are important, then peroxidic and hydroperoxidic intermediates formed by reactions of alkyl radicals with dioxygen should be involved (56–58)



It was interesting, therefore, to find (59) that halogenated porphyrins are highly active catalysts for the decomposition of alkyl hydroperoxides to form alcohols in a selective manner (see Table 7):

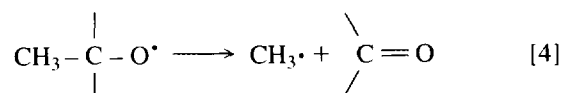


In addition, the more highly halogenated the porphyrin macrocycle, the greater the activity of the metallopor-

phyrin catalyst for this reaction. Thus, as shown in Fig. 3 and Table 7, the greater the Fe(III)/Fe(II) reduction potential, the greater the rate of alkane oxidation and the greater the rate of hydroperoxide decomposition. We have proposed (59) that a modified Haber–Weiss cycle (Fig. 6-2), creates the alkoxy and alkylperoxy radicals that lead to the stable products of decomposition: ROH and oxygen (Fig. 6-3). A kinetic analysis of these data (60) by Labinger has shown that such a pathway, with the slow step being the reduction of Fe(III) to Fe(II) by alkyl hydroperoxide, could account for rapid TBA formation during autooxidation when electron-deficient porphyrins with high Fe(III)/Fe(II) reduction potentials are used as catalysts. In fact, Labinger's analysis suggests that the majority of the isobutane oxidation reaction may proceed through a metalloporphyrin-assisted radical chain rather than a purely catalytic reaction mechanism.

Alkane Structure and Product Profile

The high selectivity observed for the oxidations of isobutane and propane shown above is not characteristic of radical reactions. The reason for this may be the low temperatures at which it is possible to conduct reactions using the highly active metallohaloporphyrin catalysts. A structural feature of these two substrates that enhances selectivity is that all carbon–carbon bonds are carbon–methyl bonds. This results in a low likelihood of C–C bond cleavage (β -scission) (61) from a possible alkoxy radical intermediate since β -scission requires the formation of an unstable methyl radical:



Thus, few carbon–carbon bond cleavage or combustion products are formed in the mild oxidations of isobutane and propane. If, on the other hand, one conducts reactions of *n*-butane with oxygen in the presence of perhalopor-

TABLE 7
Relationship between Catalyst Reduction Potential^a and Hydroperoxide Decomposition Activity^b

Catalyst	Time (h)	<i>t</i> -BuO ₂ H Conversion (%)	Product molar selectivity (%)			Fe(III)/(II) ^a E _{1/2} (V)	TBA yield at 0.5 h (%)
			<i>t</i> -BuOH	(<i>t</i> -BuO) ₂	(CH ₃) ₂ CO		
Fe(acac) ₃	2.3	<5	67	tr	32		
Fe(TPP)Cl	1.9	27	82	7	11	-0.221	4.8
Fe(TPPF ₂₀)Cl	3.3	72	87	10	3	+0.07	16.0
Fe(TPPF ₂₀ β -Br ₈)Cl	1.9	95	90	8	2	+0.19	52.2
Fe(TPPF ₂₀ β -Cl ₈)Cl	3.3	100	90	8	2	+0.28	67.2

^a Cyclic voltammetry in CH₂Cl₂ vs SCE, TBAC-supporting electrolyte, glassy carbon electrode.

^b The catalyst, 2×10^{-4} mmol, in 2.4-ml *p*-xylene was rapidly added to a stirred solution of 10 ml *t*-BuO₂H (90%) in 48 ml benzene at 25°C. O₂ evolved was measured manometrically and liquid samples taken periodically and analyzed by standardized GC.

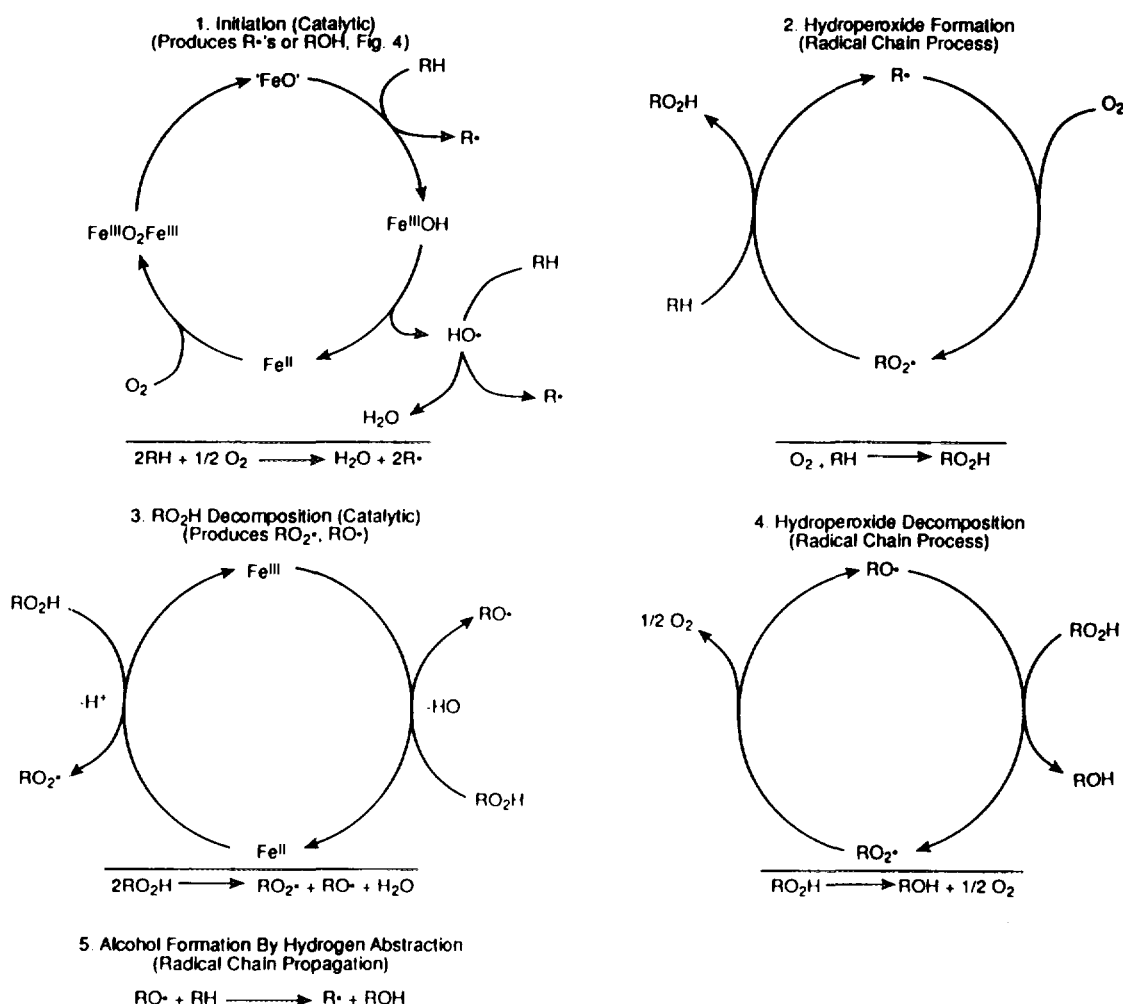


FIG. 6. Possible pathways occurring during selective oxidation of alkanes catalyzed by iron perhaloporphyrin complexes.

phyrin complexes, significant oxidative cleavage results, forming by-products such as acetic acid and acetaldehyde (Table 8). It is of interest to note that selectivity to 2-butanone is enhanced over those of iron by chromium complexes. The azido form of the chromium complex is most effective for generating ketones *via* alkane oxidations. Oxidations carried out in the presence of this catalyst are very rapid and exhibit the characteristic sigmoid kinetic curve of autooxidations, including the presence of a substantial induction period.

Table 9 details the product profiles for the oxidations of a series of branched alkanes with 3° C–H bonds and Fig. 7 summarizes the dependence of the product profile on substrate structure for oxidations catalyzed by tetrakis(pentafluorophenyl β-octabromo)porphyrinatoiron (III)hydroxide. Those hydrocarbons having tertiary C–H bonds react at temperatures of 60°C or less while those having secondary but no tertiary C–H bonds require more elevated temperatures and primary C–H bonds have very

low reactivity at any of the temperatures used. The relative C–H bond reactivity pattern: 3° > 2° > 1° is consistent with that of radical-initiated oxidation pathways (1b, 49, 50, 62).

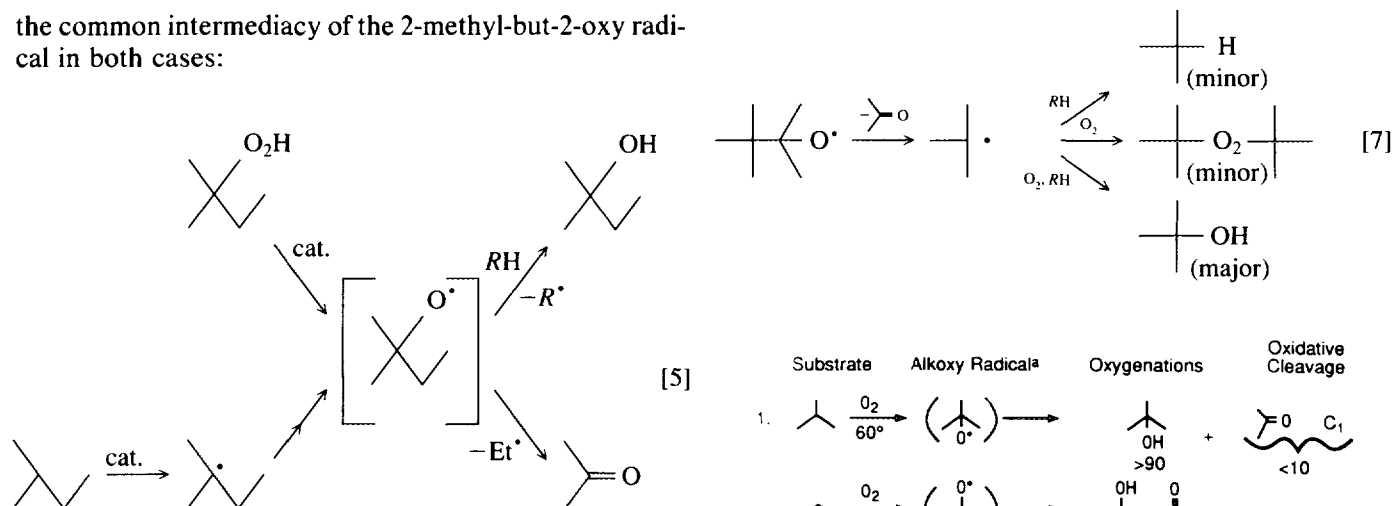
The ratio of selective oxidation to cleavage products in the case of propane or isobutane oxidations is ~9/1. On the other hand, the ratio of four- or five-carbon oxidation products to cleavage products is less than 2/1 in oxidations of *n*-butane and 2-methylbutane, respectively, and when 3-methylpentane is oxidized, the oxygenation/cleavage ratio drops below 1. It is interesting in this regard that decomposition of *tert*-amyl hydroperoxide (TAHP) (Table 10), leads to a far greater extent of carbon–carbon bond cleavage than does decomposition of *tert*-butyl hydroperoxide (Table 7). Furthermore, the ratio of *tert*-amyl alcohol to acetone produced during catalyzed TAHP decomposition in benzene at room temperature is very similar to the ratio of these products formed via 2-methyl butane oxidation (Table 9). This observation is consistent with

TABLE 8
n-Butane Oxidations Catalyzed by TPPF₂₀β-Cl₈ Complexes of Iron and Chromium^a

Catalyst	Solvent	Reaction time (h)	TO	Oxidation product molar selectivity (%)			
				SBA (2-C ₄ H ₉ OH)	MEK (2-C ₄ H ₈ O)	Acetaldehyde (CH ₃ CHO)	Acetic acid (CH ₃ CO ₂ H)
Fe(TPPF ₂₀ β-Cl ₈)Cl	Benzene	4.5	243	28	56	tr	15
Cr(TPPF ₂₀ β-Cl ₈)Cl	Benzene	5.5	9	40	60	—	—
	Benzene	23.0	711	10	60	3	27
	Acetonitrile	23.0	1518	7	48	5	40
Cr(TPPF ₂₀ β-Cl ₈)N ₃	Benzene	2.2	659	7	64	4	25
	Acetonitrile	3.5	1508	12	51	3	34

^a Butane (60 g) in 48 ml of the solvent containing 0.023 mmol catalyst was oxidized at 125°C under 1500 psig of air.

the common intermediacy of the 2-methyl-but-2-oxo radical in both cases:



When the symmetrical hydrocarbon 2,3-dimethylbutane is used, a substrate having two easily abstractable 3° C-H bonds and an isopropyl group adjacent to either internal carbon atom, cleavage predominates over six-carbon oxidation products by a wide margin.

Thus, by varying the structure of the alkane substrate we are able to move from selective oxygenations that retain the intact carbon skeleton and give only 10% carbon-carbon bond cleavage or less, to greater than 90% C-C bond cleavage reactions in these alkane oxidations. *The direction of the effect of alkane structure on carbon-carbon bond scission is consistent with the intermediacy of alkoxy radicals as significant reaction intermediates* (61, 62).

Iron-haloporphyrin-catalyzed oxidation of 2,2,3-trimethylbutane

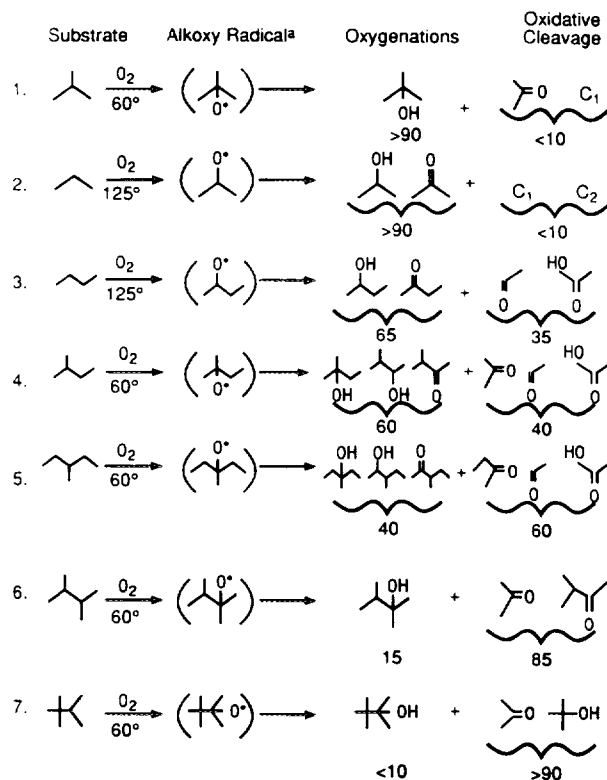
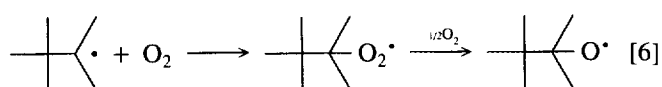
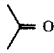
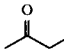
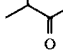
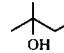
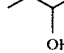
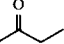
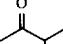
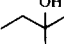
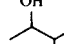
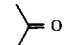
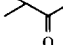
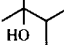
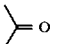
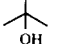


FIG. 7. Dependence of product profile on substrate structure for alkane oxidations catalyzed by Fe(TPPF₂₀β-Br₈)OH. (a) Hypothetical alkoxy radical.

TABLE 9
Alkane Oxidations Catalyzed by Iron Halotetraphenylporphyrins^a

Alkane	Catalyst	T (°C)	TO ^b	Products (mmol/100 g reaction mix) ^c					Oxygenation/ cleavage ^d
									
2-Methylbutane	Fe(TPPF ₂₀)OH	40	105	2.9	0.4	1.1	5.8	0.3	2.2
	Fe(TPPF ₂₀ β-Br ₈)Cl	40	195	3.0	0.5	1.9	8.9	0.3	3.2
	Fe(TPPF ₂₀)OH	60	670	12.8	1.0	3.3	13.2	0.8	1.3
	Fe(TPPF ₂₀ β-Br ₈)Cl	60	980	21.6	2.7	6.3	25.4	1.2	1.4
	Fe(TPPF ₂₀)Cl	80	2110	55.3	3.5	11.3	32.5	2.0	0.8
	Fe(TPPF ₂₀ β-Br ₈)Cl	80	3200	61.3	4.0	14.8	41.4	2.3	0.9
				Products (mmol/100 g reaction mix) ^c					
				AA ^e					
3-Methylpentane	Fe(TPPF ₂₀ β-Br ₈)Cl	80	1556	na	28.9	11.5	14.1	2.0	na
	Fe(TPPF ₂₀ β-Br ₈)Cl	80	1556	19.0	28.1	11.2	13.4	1.9	0.56
				Products (mmol/100 g reaction mix) ^c					
									
2,3-Dimethylbutane	Fe(TPPF ₂₀ β-Br ₈)Cl	60	2245		120.4	10.3	22.3		0.17
	Fe(TPPF ₂₀ β-Br ₈)Cl	80	5650		329.0	22.0	40.0		0.11
				Products (mmol/100 g reaction mix) ^c					
						C ₇ H ₁₅ OH			
2,2,3-Trimethylbutane	Fe(TPPF ₂₀)OH	60	1310		30.1	26	2.8		0.09
	Fe(TPPF ₂₀ β-Cl ₈)OH	60	1490		23.3	20.1	1.9		0.08

^a Oxidations carried out by reacting oxygen with the neat alkane (30 ml), containing 0.013 mmol of the catalyst at T (°C) at a total pressure of 100 psig for 6 h. Product analysis by standardized GLPC.

^b Mol O₂ consumed/mol catalyst used.

^c mmol product/100 g of recovered product mixture, by GLPC.

^d Ratio of mol oxidation products with carbon skeleton intact/mol C–C bond cleavage products.

^e AA, acetic acid.

gives rise to equimolar amounts of acetone and products of the very stable *tert*-butyl radical. The hypothetical alkoxy radical in this case would cleave nearly exclusively, giving very little C₇ oxygenate.

Greene and co-workers (62) have demonstrated that the ratio of rates of alkyl cleavage from alkoxy radicals vs H abstraction from cyclohexane at 40°C increases dramatically from methyl to ethyl to isopropyl. In Table 11 we compare the percentage of cleavage products formed during catalytic oxidations at 60 and 80°C with this ratio and find qualitative similarities. Differences arise since H-abstraction in the oxidation cases would be largely from 3° C–H rather than from 2° C–H bonds. Nonetheless,


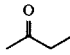
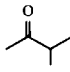
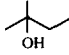
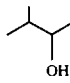
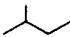
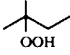
there is clear directional similarity between the extent of intramolecular C–C bond cleavage reactions from alkoxy radicals and the selectivity of metalloporphyrin-catalyzed oxidations that we have conducted.

CONCLUSIONS

Halogenated metalloporphyrin complexes are extremely active catalysts for the selective oxidation of alkanes and the decomposition of alkylhydroperoxides to alcohols. Perhalotetraphenylporphyrinatoiron complexes are the most active catalysts known for both of these reactions, giving rates an order of magnitude greater than

TABLE 10

Comparison of the Product Profile of 2-Methylpentane Oxidation^a with That of *tert*-Amyl Hydroperoxide Decomposition Catalyzed by Perhaloporphyrinatoiron Complexes

Substrate	Reaction	TO	Products (mmol/100 g reaction mix)					MB-2ol/ acetone ^b
								
	Oxidation ^a	195	3.0	0.5	1.9	8.9	0.3	3
	Decomposition ^c	3.3×10^5	33.4	4.5	—	116.8	—	3.5

^a Oxygen is reacted with the neat alkane (30 ml) containing 0.013 mmol of Fe(TPPF₂₀β-Br₈)OH at 40°C at a total pressure of 100 psig for 6 h. Product analysis by standardized GLPC.

^b 2-MB-2ol/acetone is the ratio of 2-methylbutane-2-ol to acetone formed in the reaction.

^c *tert*-Amyl hydroperoxide, 10 ml (82%), is added to a solution of Fe(TPPF₂₀βCl₈)Cl (4×10^{-6} M) in benzene. Oxygen evolution is followed manometrically and products are analyzed periodically by standardized GLPC. The analysis was performed after 1.9 h.

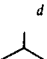
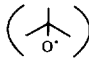
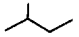
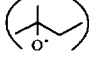
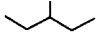
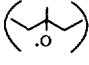
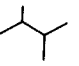
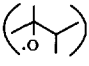
any previously reported (73). The low temperatures at which these oxidations can be conducted result in some unique and useful selectivities.

Although biomimetic chemistry may be involved in initiation of radical chains (Fig. 5d), and indeed in a degree

of dioxygenase-like catalysis (Fig. 5e), decomposition of peroxidic intermediates by iron perhaloporphyrin catalysts is also of great importance. The bulk of the available evidence indicates that radical chain processes are occurring. Figure 6 indicates a possible scheme in which the

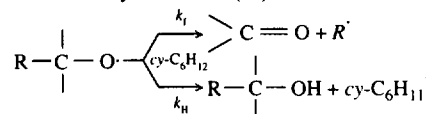
TABLE 11

Product Profile as a Function of *R* in Oxidation of R₁R₂R₃CH Catalyzed by Fe(TPPF₂₀β-Br₈)Cl^a

Alkane	R ₁	R ₂	R ₃	Predominant hypothetical alkoxy radical	Predominant cleaved alkyl radical	k _f /k _H ^b	Cleavage products formed in oxidation (%) ^c
	CH ₃	CH ₃	CH ₃		CH ₃	0.021	10
	CH ₃	CH ₃	C ₂ H ₅		C ₂ H ₅	2.09	53
	CH ₃	C ₂ H ₅	C ₂ H ₅		(2)C ₂ H ₅		64
	CH ₃	CH ₃	<i>i</i> -C ₃ H ₇		(CH ₃) ₂ CH	76.4	90

^a Oxidations carried out by reacting oxygen with the neat alkane (30 ml) containing 0.013 mmol of Fe(TPPF₂₀β-Br₈)Cl at 80°C at a total pressure of 100 psig for 6 h. Product analysis by standardized GLPC.

^b Ratio of rates of alkyl cleavage and H-abstraction from cyclohexane (61) in the reaction:



^c (Mol alkane converted to C-C bond cleavage products/mol alkane oxidized) × 100.

^d A 25 wt% solution of isobutane in benzene was oxidized in this experiment.

metal complexes initiate formation of radicals, 1, that generate hydroperoxides, 2, which are catalytically converted to radicals, 3, that produce stable oxidation products, 4. If this is so, then the majority of the alcohol produced in the oxidation of isobutane, for example, would arise by hydrogen abstraction, 5, rather than by biomimetic rebound (Fig. 4e). It seems likely that all of these processes are proceeding in these oxidations and further work will sort out the relative importance of each.

EXPERIMENTAL

General. ^1H NMR (Bruker MSL 300 MHz), ^{19}F NMR (Nicolet NT-300 300 MHz), IR spectra (Mattson R/S FTIR), absorption spectra (HP 8452A), and ion cyclotron resonance mass spectra (Nicolet FTMS) were collected routinely. Fast atom bombardment mass spectra were collected by M-Scan, Inc. (West Chester, PA). Laser desorption mass spectra were collected at the University of Delaware on a Nicolet LD-FTMS 2000 instrument.

Solvents. All solvents used were HPLC grade from Aldrich and were used as purchased unless further purification is noted. The CHCl_3 used contained 0.75% ethanol unless it is noted that ethanol-free CHCl_3 was used.

Reagents. All nonporphyrin reagents were purchased from Aldrich, unless noted, and were certified ACS reagent grade or better. FeTPPCl , $\text{MnTPP}(\text{OAc})$, and $(\text{FeTPP})_2\text{O}$ were purchased from Strem Chemicals. $\text{FeTPPF}_{20}\text{Cl}$ and $\text{H}_2\text{TPPF}_{20}$ were purchased from Aldrich. $\text{Fe}(\text{TPP}\text{Cl}_8\beta\text{-Br}_4)\text{Cl}$ was purchased from Midcentury Chemicals. CrTPPCl (63), MnTPPN_3 and CrTPPN_3 (64), FeTPPN_3 (65), $[\text{Fe}(\text{TPP}\beta\text{-Br}_4)]_2\text{O}$ (66), $\text{Fe}(\text{TPP}\beta\text{-Br}_4)\text{Cl}$ (67), $\text{Fe}(\text{TPP}\text{Cl}_8)\text{Cl}$ and $\text{Fe}(\text{TPP}\text{Cl}_8)\text{OH}$ (68), $\text{Fe}(\text{TPPF}_{20})\text{OH}$ and $(\text{FeTPPF}_{20})_2\text{O}$ (69), $\text{Cr}(\text{TPPF}_{20})\text{Cl}$ (70), $\text{Mn}(\text{TPPF}_{20})\text{OAc}$ (71), $\text{Co}(\text{BPI})\text{OAc}$ (72), and $\text{Co}(\text{BPI})(\text{O}_2\text{Bu}^t)$ (40) were made by the referenced methods.

Oxidation methods. Oxidations were carried out either in 60-cc Fisher-Porter aerosol tubes or in 300- to 500-ml batch autoclaves as indicated in the tables. Reactions run in Fisher-Porter tubes, equipped with a baffled magnetic stirrer, were carried out at 100 psig total pressure at the temperatures indicated in the tables. The catalyst was dissolved in either the neat alkane or in a benzene solution to which the alkane was added. The Fisher-Porter tube was attached to a manifold for adding and releasing gases. Oxygen was admitted to the tube and the tube was then submerged in a constant temperature bath at reaction temperature. The reaction mixture was magnetically stirred for the amount of time indicated in the table. Gas uptake was measured by a pressure gauge and oxygen was replenished as it was consumed. At the time indicated in the table, the tube was removed from the bath, cooled

to 0°C , and the gas slowly vented. The liquid product was weighed and analyzed by standardized GLPC. *Caution: Many of the reactions conducted in this work were done within the explosion range. Reactions were performed in a properly barricaded laboratory area for safety.*

Propane oxidations were routinely performed in a glass-lined 300-ml stainless steel autoclave fitted with thermocouple and magnedrive stirrer. All internal parts, including cooling coils, thermocouple, and stirrer blades and shaft, were coated with Teflon. A solution of the catalyst in benzene was added to the glass liner, the autoclave was secured, and liquid propane was pumped into the reactor. Air was added to a total pressure of 1500 psig and the reactor heated to reaction temperature. After the reaction time indicated in the tables, the reactor was cooled to room temperature, gases were slowly vented into a gas bag for GLPC analysis, and the liquid product was analyzed by standardized GLPC.

Hydroperoxide decompositions. A solution of the catalyst in *p*-xylene (internal standard) was quickly added to a rapidly stirred solution of *tert*-butyl hydroperoxide in benzene at room temperature. Oxygen evolution was measured manometrically and liquid products were analyzed periodically by standardized gas chromatography. *Caution: Reactions should be run in dilute solutions of catalyst and/or hydroperoxide to avoid exotherms and dangerously fast gas evolution.*

Benzene (99.99%, Aldrich), *tert*-butyl alcohol (99.6%, Aldrich), and *p*-xylene (99+%, Aldrich) were used as purchased. *tert*-Butyl hydroperoxide (90%, 5% water, 5% *tert*-butyl alcohol) was used as purchased from Aldrich.

$\text{Mn}(\text{TPPF}_{20})\text{N}_3$. $\text{Mn}(\text{TPPF}_{20})\text{OAc}$ (0.4 g) is dissolved in 40 ml of CHCl_3 . Ten milliliters of saturated aqueous NaN_3 solution is stirred vigorously with the CHCl_3 solution overnight. The water layer is separated and 10 ml of fresh NaN_3 solution is added and stirred again overnight. The water layer is removed and the CHCl_3 is washed three times with 20 ml of H_2O . The CHCl_3 solution is dried over Na_2SO_4 , then filtered and rotovapped to dryness. This material is washed with copious amounts of H_2O then dried overnight under vacuum over P_2O_5 at 60° . Yield 0.36 g. IR shows a N-N stretch at 2030 cm^{-1} .

$\text{Cr}(\text{TPPF}_{20})\text{N}_3$. $\text{Cr}(\text{TPPF}_{20})\text{Cl}$ (400 mg) is dissolved in 100 ml of acetone. NaN_3 (4.0 g) is added and the mixture is stirred for 48 h at room temperature. After the solvent is removed and the solid product is washed with H_2O and dried, a yield of 350 mg of $\text{Cr}(\text{TPPF}_{20})\text{N}_3$ is obtained. IR(KBr) shows a N-N stretch at 2053 cm^{-1} .

$\text{Fe}(\text{TPPF}_{20})\text{N}_3$. $\text{Fe}(\text{TPPF}_{20})\text{Cl}$ (0.5 g) is dissolved in 100 ml of acetone and 5.0 g of NaN_3 is added. Most of the NaN_3 and all of the $\text{Fe}(\text{TPPF}_{20})\text{Cl}$ is dissolved. This mixture is stirred at room temperature for 24 h, then

filtered and rotovapped to dryness. The material is washed with large amounts of H₂O, then vacuum-dried overnight at 60°. Yield 0.4 g. IR shows a (N–N) stretch of azide at 2053 cm⁻¹. Large crystals are grown by recrystallization in 5% hexane in chloroform.

Fe(TPPF₂₀β-Br₈)Cl. Under N₂. 0.500 g of Fe(TPPF₂₀)Cl is dissolved in 300 ml of degassed CCl₄ which is freshly distilled (over P₂O₅). One-hundred milliliters of 6 M Br₂/CCl₄ is added quickly to this solution while at reflux. After 18 h the Soret absorption has moved from 418 to 429 nm. An additional 50 ml of 6 M Br₂ in CCl₄ is added at this point. After several more hours of reflux, the Soret absorption remains at 429 nm. The solution is cooled, filtered and washed three times with H₂O, and then evaporated to dryness. The greenish-brown material is chromatographed on neutral alumina eluting with CHCl₃. The first green band is collected, treated with dilute HCl, and evaporated to dryness. After drying *in vacuo* at 110°C, 590 mg of the Fe(TPPF₂₀β-Br₈)Cl is obtained. FAB/MS: M⁺-Cl 1659.

Fe(TPPF₂₀β-Br₈)N₃. Fe(TPPF₂₀β-Br₈)Cl (300 mg) is dissolved in 300 ml of methanol and 200 ml of acetone. To this solution is added 3.5 g of NaN₃ and then 10 drops of glacial acetic acid. The solution is stirred for 72 h and then filtered; the solvent is removed by rotary evaporation. The dry material is washed with water and dried *in vacuo* at room temperature. Yield is quantitative. IR(KBr): ν_{N-N} 2049 cm⁻¹.

Cr(TPPF₂₀β-Br₈)Cl. Under N₂, 0.700 g of Cr(TPPF₂₀)Cl is dissolved in 600 ml of freshly distilled (over P₂O₅) CCl₄. The solution is heated to 40°C and 150 ml of Br₂ is added dropwise with stirring. The Soret absorption of the unreacted chromium porphyrin at 436 nm shifts to 481 nm after 22 h reaction time. At this point, the solution is cooled, filtered and washed three times with water, and then evaporated to dryness. The green material is redissolved in a minimum of CHCl₃ and chromatographed on neutral alumina. The solution is washed with 1 N HCl and then evaporated to dryness. Yield 350 mg. UV/VIS (toluene): 400, 483, 599 nm.

Cr(TPPF₂₀β-Br₈)N₃. Cr(TPPF₂₀β-Br₈)Cl (300 mg) is dissolved in 300 ml of methanol and 200 ml of acetone. To this solution is added 3.5 g of NaN₃; the solution is then stirred for 48 h. After being filtered, the solvent is removed with a rotary evaporator and the solids are washed with water and dried *in vacuo* at room temperature. Yield 260 mg. IR(KBr): ν_{N-N} 2050 cm⁻¹.

Mn(TPPF₂₀β-Br₈)Cl. Mn(TPPF₂₀)Cl (0.400 g) is dissolved in 300 ml of freshly distilled (over P₂O₅) CCl₄ under N₂. The solution is warmed and 125 ml of Br₂ is added dropwise with stirring. The reaction is continued until a sample shows a Soret of greater than 450 nm. After being

washed three times with water, the solvent is evaporated. The material is dissolved in a minimum of CHCl₃ and chromatographed on neutral alumina. The CHCl₃ solution is washed with 1 N HCl and then evaporated to dryness. Yield 320 mg. UV/VIS (Toluene): 399, 452, 495, 603 nm.

Mn(TPPF₂₀β-Br₈)N₃. Mn(TPPF₂₀β-Br₈)Cl (150 mg) is dissolved in 150 ml of methanol and 100 ml of acetone. NaN₃ (1.5 g) is added and the mixture is stirred for 48 h. After filtration and removal of the solvent, the solids are washed with water. Yield 130 mg. IR(KBr): ν_{N-N} 2037 cm⁻¹.

H₂TPPF₂₀β-Cl₈. The preparation of this porphyrin is accomplished by the chlorination of ZnTPPF₂₀ with Cl₂ and *in situ* removal of Zn with HCl.

A three-necked flask fitted with a reflux condenser and a N₂ inlet port is charged with 1.0 g (0.96 mmol) of Zn(TPPF₂₀) and 500 ml CCl₄ degassed previously with N₂. The N₂ flow is terminated and Cl₂ is bubbled through the solution slowly for 4 min while the solution is refluxed. After 4 min, the Cl₂ flow is stopped and N₂ is used above the condenser to blanket the apparatus. After 1 h of reflux an aliquot is removed and the Soret absorption is checked. The reaction is complete when the Soret reaches 448 nm. If the reaction is incomplete then a second 4-min Cl₂ addition is performed, followed by 1 h of additional reflux. The solution is allowed to cool to 60°, and then HCl gas is bubbled through the hot solution for 2 min and stirred for 15 min more. TLC (silica gel, CH₂Cl₂) is used to check that the Zn removal is complete. The green solution is cooled, washed with 200 ml of 5% NaHCO₃, and then the solvent is removed by rotary evaporation. Chromatography on neutral alumina eluting with CHCl₃ gave 1.28 g (71% yield). LDMS: M⁺ = 1250. ¹⁹F NMR (CDCl₃, 282.307 MHz referenced to C₆D₅F): δ - 136.88 (m, 8F, *o*-ArF), -148.34 (t, 4F, *p*-ArF), -160.50 (m, 8F, *m*-ArF).

Fe(TPPF₂₀β-Cl₈)Cl. A 250-ml flask is charged with 750 mg of H₂TPPF₂₀β-Cl₈, 200 ml of DMF, and 10 ml of acetic acid. After being heated to 160° under N₂, 240 mg of powdered FeCl₂ · 4H₂O is added with stirring. After 10–15 min, the solution is cooled and poured into 200 ml of H₂O. After standing overnight, the mixture is filtered and the solids dissolved in CHCl₃ and chromatographed on alumina eluting with CHCl₃, giving 580 mg (72% yield) after treatment with Na₂SO₄ and after being dried. ¹⁹F NMR (CDCl₃ referenced to C₆D₅F): δ - 114.4, -119.2 (broad resonances, 8F, *o*-ArF), -148.4 (4F, *p*-ArF), 157.1 (8F, *m*-ArF). LDMS: M-Cl⁺ 1304, M⁺ 1339.

Fe(TPPF₂₀β-Cl₈)N₃. This azide complex is prepared by reacting 100 mg of Fe(TPPF₂₀β-Cl₈)Cl with 1.0 g of NaN₃ in 200 ml of acetone with vigorous stirring for 24 h. The product mixture is filtered. The filtrate is evaporated to dryness and the remaining solid is washed with

water. The solid product is then dried *in vacuo* at 70°C. The infrared spectrum shows a sharp ν_{N-N} stretch at 2037 cm^{-1} .

Cr(TPPF₂₀ β -Cl₈)Cl. A 250-ml flask containing a solution of H₂ TPPF₂₀ β -Cl₈ (750 mg, 0.60 mmol) in 200 ml DMF under a nitrogen atmosphere is placed in an oil bath preheated to 160°C. After the solution starts refluxing, Cr(CO)₆ (132 mg, 0.60 mmol) is added every 30 min until the chromium insertion is judged to be complete by TLC. The reaction mixture is cooled to room temperature under a N₂ atmosphere. At this point the solution is poured into 200 ml of cold saturated NaCl solution and stirred for 10 min. The brown flocculate is isolated from the aqueous solution by vacuum filtration. The resulting brown paste is dissolved in 20 ml CHCl₃ and chromatographed on Al₂O₃ with CHCl₃ steadily enriched with methanol. The product is the second porphyrin component which came off the column and eluted as a broad red-brown band and is treated in the normal fashion with 1 N HCl. The solvent is removed by rotary evaporation to give Cr(TPPF₂₀ β -Cl₈)Cl in 30% yield. LDMS: M^- -Cl 1299, M^+ 1336. UV/VIS (CHCl₃): 432 nm.

Cr(TPPF₂₀ β -Cl₈)N₃. The complex Cr(TPPF₂₀ β -Cl₈)Cl (96 mg) and sodium azide (1.0 g) are stirred in 200 ml of acetone at room temperature for 72 h under nitrogen and then the solution is filtered. The filtrate is evaporated to dryness giving a solid product which is washed thoroughly with water and dried *in vacuo*. The purple azide complex (ν_{N-N} 2055 cm^{-1}) is recovered in quantitative yield. UV/VIS (CHCl₃): 418, 440 nm.

Mn(TPPF₂₀ β -Cl₈)Cl. The free base H₂TPPF₂₀ β -Cl₈ (300 mg) is dissolved in 33 ml of DMF. The solution is stirred at reflux under nitrogen for 15 min. At this point Mn(OAc)₂ · 4H₂O (200 mg) is added and the mixture is stirred at reflux under nitrogen for an additional 30 min. An additional 50 mg of Mn(OAc)₂ · 4H₂O is added and the mixture refluxed for an additional 30 min. At this point an aliquot is taken, evaporated to dryness, and the solid taken up in CHCl₃. A TLC check of this solution reveals no starting porphyrin. The DMF solution of manganese complex is then allowed to cool to room temperature and added to 50 ml of a 30 wt% solution of sodium chloride in water. The mixture is refrigerated overnight, during which time the product precipitates from solution. The solid product is washed with water (5 × 20 ml), filtered, air dried for an hour, then dissolved in a minimum of CHCl₃. The CHCl₃ solution is chromatographed on alumina; then the product is taken to dryness in a rotary evaporator. The solid product is dried at 80°C in a vacuum oven; 240 mg of product is recovered, having a Soret at 450 nm.

Mn(TPPF₂₀ β -Cl₈)N₃. A round-bottom flask under N₂ is charged with 100 mg of Mn(TPPF₂₀ β -Cl₈)Cl, 300 ml of

acetone, 50 ml of methanol, and 1.0 g of NaN₃. This mixture is stirred vigorously at room temperature for 12 h, filtered, and the solvent removed by rotary evaporation. The solids are dissolved in 50 ml of CH₂Cl₂ and washed twice with 25 ml of H₂O, after which the organic layer is dried over Na₂SO₄. The solvent is removed by rotary evaporation and the purple solids dried *in vacuo* overnight at room temperature. The yield is quantitative. IR(KBr): ν_{N-N} = 2031 cm^{-1} with a shoulder at 2066 cm^{-1} .

Co(TPPF₂₀ β -Cl₈). A stirred solution of 200 mg of Co(OAc)₂ · 4H₂O in 50 ml of DMF is heated to 140° in an oil bath; then 250 mg of the free base H₂TPPF₂₀ β -Cl₈ is added as a powder all at once. After 15 min, an aliquot is taken, evaporated to dryness, and a TLC check is made on alumina eluting with CHCl₃. No free base is seen by TLC. The total reaction time is limited to 30 min. The contents of the flask are cooled quickly to room temperature and added to an equal volume of saturated NaCl solution. The resulting precipitate was filtered, giving a reddish-brown paste which is redissolved in CHCl₃ and chromatographed on neutral alumina eluting with CHCl₃. After evaporation of the solvent and drying *in vacuo* at 110°, 210 mg of the product is obtained. UV/VIS(CHCl₃): 427, 552, 578 nm. LDMS: M^+ 1307.

Co(BPI)N₃. In an Erlenmeyer flask under N₂ is stirred 0.5 g of Co(BPI)(OAc) in 200 ml of methanol. At reflux 0.6 g of NaN₃ is added and reflux is continued for 1 h. After being cooled and filtered, the volume is reduced to 100 ml, and then an equal volume of ether is added to precipitate the product, which is washed with water, washed with ether, and then dried *in vacuo* overnight at room temperature. The yield is quantitative. IR(KBr): ν_{N-N} = 2015 cm^{-1} .

Fe(TPP β -Br₄)N₃. A round-bottomed flask under N₂ is charged with 100 mg of Fe(TPP β -Br₄)Cl and 100 ml of CHCl₃. With stirring, 1.0 g of NaN₃ in 50 ml of H₂O and 5 drops of H₂SO₄ is added. After stirring for 12 h the CHCl₃ is separated, filtered, and washed twice with water. The CHCl₃ layer is reduced in volume by rotary evaporation until a precipitate forms. The material is filtered and washed with H₂O, then dried *in vacuo*. Yield 90 mg. UV/VIS (CHCl₃): 433, 523, 602 nm. IR(KBr): ν_{N-N} = 2030 cm^{-1} .

Fe(TPPCl₈)N₃. Fe(TPPCl₈)Cl (200 mg) is dissolved in 100 ml of CHCl₃ in an Erlenmeyer flask under N₂. Two grams of NaN₃ dissolved in 40 ml of H₂O and 5 drops of H₂SO₄ is added. This two-phase mixture is stirred vigorously for 24 h; then the CHCl₃ layer is separated, dried over Na₂SO₄, and evaporated to dryness. The purple solids are washed with water and dried *in vacuo*. Yield 150 mg. IR(KBr): ν_{N-N} = 2055 cm^{-1} .

$Fe(TPPCl_8\beta-Br_4)N_3$. A 100-mg quantity of Fe($TPPCl_8\beta-Br_4$)Cl is dissolved in 100 ml of $CHCl_3$ and 1.0 g of NaN_3 dissolved in 20 ml of H_2O with a few drops of H_2SO_4 is added. This two-phase mixture is stirred vigorously for 24 h; then the organic layer is separated, washed twice with H_2O , and dried over Na_2SO_4 . After removal of the solvent, the solids were washed with H_2O and dried *in vacuo* at room temperature. The yield is 80 mg of purple powder. IR(KBr): $\nu_{N-N} = 2050\text{ cm}^{-1}$.

ACKNOWLEDGMENTS

Financial assistance from the U.S. Department of Energy (Morgantown Energy Technology Center), the Gas Research Institute, and Sun Co. is greatly appreciated.

REFERENCES

- (a) Lyons, J. E., "Surface Organometallic Chemistry: Molecular Approaches to Surface Catalysis" (J. M. Basset, Ed.), p. 97. Kluwer Academic, Dordrecht/Norwell, MA, 1988; (b) Lyons, J. E., "Applied Industrial Catalysis" (B. E. Leach, Ed.), Chap. 6, Vol. 3, p. 131. Academic Press, New York, 1984; (c) Lyons, J. E., *Hydrocarbon Process.*, 107 (1980).
- Groves, J. T., Nemo, T. E., and Myers, R. S., *J. Am. Chem. Soc.* **98**, 859 (1976).
- Groves, J. T., Nemo, T. E., and Myers, R. S., *J. Am. Chem. Soc.* **101**, 1032 (1979).
- Groves, J. T., and Kruper, W. J., Jr., *J. Am. Chem. Soc.* **101**, 7613 (1979).
- Meunier, B., *Chem. Rev.* **92**, 1411 (1992).
- Mansuy, D., Bartoli, J. F., Chottard, J. C., and Lange, M., *Agnew. Chem. Int. Ed. Eng.* **19**, 909 (1980).
- Hill, C. L., and Schardt, B. C., *J. Am. Chem. Soc.* **102**, 6374 (1980).
- Chang, C. K., and Ebina, F., *J. Chem. Soc. Chem. Commun.*, 778 (1981).
- Groves, T., and Nemo, T. E., *J. Am. Chem. Soc.* **105**, 6243 (1983).
- DePorter, B., Ricci, M., Bortolino, O., and Meunier, B., *J. Mol. Catal.* **31**, 221 (1985).
- Tabushi, I., and Yazaki, A., *J. Am. Chem. Soc.* **103**, 7371 (1981).
- Tabushi, I., and Koga, N., *J. Am. Chem. Soc.* **101**, 6456 (1979).
- Tabushi, I., *Coord. Chem. Rev.* **86**, 1 (1988).
- Mansuy, D., Fontecave, M., and Bartoli, J. F., *J. Chem. Soc. Chem. Commun.*, 253 (1983).
- Fontecave, M., and Mansuy, D., *Tetrahedron* **40**, 4297 (1984).
- Ji, L., Liu, M., Hsieh, A. K., and Hor, T. S. A., *J. Mol. Catal.* **70**, 247 (1991).
- Iwanejko, R., Mlodnicka, T., and Poltowicz, J., "New Developments in Selective Oxidation" (G. Centi and F. Trifiro, Eds.), p. 195. Elsevier, Amsterdam, 1990.
- Battioni, P., Bartoli, J. F., Leduc, P., Fontecave, M., and Mansuy, D., *J. Chem. Soc. Chem. Commun.*, 791 (1987).
- Karasevich, E. I., Khenkin, A. M., and Shilov, A. E., *J. Chem. Soc. Chem. Commun.*, 731 (1987).
- Shulpin, G. B., and Druzhinina, A. N., *Izv. Akad. Nauk SSSR Ser. Khim.* 2739 (1991).
- Leduc, P., Battioni, P., Bartoli, J. F., and Mansuy, D., *Tetrahedron Lett.* **29**, 205 (1988).
- Bedioui, F., Granados, S. G., and Devynck, J., *New J. Chem.* **15**, 939 (1991).
- Hendrickson, D. N., Kinnaird, M. G., and Suslick, K. S., *J. Am. Chem. Soc.* **109**, 1243 (1987).
- Maldotti, A., Bartocci, C., Amadelli, R., Polo, E., Battioni, P., and Mansuy, D., *J. Chem. Soc. Chem. Commun.*, 1487 (1991).
- Ellis, P. E., Jr., and Lyons, J. E., *J. Chem. Soc. Chem. Commun.*, 1188 (1989).
- Ellis, P. E., Jr., and Lyons, J. E., *J. Chem. Soc. Chem. Commun.*, 1190 (1989).
- Ellis, P. E., Jr., and Lyons, J. E., *J. Chem. Soc. Chem. Commun.*, 1316 (1989).
- Ellis, P. E., Jr., and Lyons, J. E., *Catal. Lett.* **3**, 389 (1989).
- Lyons, J. E., and Ellis, P. E., Jr., *Catal. Lett.* **8**, 45 (1991).
- Ellis, P. E., Jr., and Lyons, J. E., *Coord. Chem. Rev.* **105**, 181 (1990).
- Lyons, J. E., Ellis, P. E., Jr., and Durante, V. A., "Studies in Surface Science and Catalysis" (R. Grasselli, Ed.), Vol. 67, p. 99. Elsevier, New York, 1991.
- Ellis, P. E., Jr., and Lyons, J. E., *Prepr. Petr. Div.* **35**, 174 (1990).
- Lyons, J. E., Ellis, P. E., Jr., Wagner, R. W., Thompson, P. B., Gray, H. B., Hughes, M. E., and Hodge, J. A., *Prepr. Petr. Div.* **37**, 307 (1992).
- Lyons, J. E., and Ellis, P. E., Jr., "Metalloporphyrins in Catalytic Oxidations" (R. A. Sheldon, Ed.), p. 291. Dekker, New York, (1994).
- Bartoli, J. F., Brigoud, O., Battioni, P., and Mansuy, D., *J. Chem. Soc. Chem. Commun.*, 440 (1991).
- Bartoli, J. F., Battioni, P., DeFoor, W. R., and Mansuy, D., *J. Chem. Soc. Chem. Commun.*, 23 (1994).
- Mansuy, D., "The Activation of Dioxygen and Homogeneous Catalytic Oxidation" (D. H. R. Barton *et al.*, Eds.), p. 347. Plenum, New York, 1993.
- Grinstaff, M. W., Hill, M. G., Labinger, J., and Gray, H. B., *Science* **264**, 1311 (1994).
- Tolman, C. A., Druliner, J. P., Krusic, P. J., Nappa, M. J., Seidel, W. C., Williams, I. D., and Ittel, S. D., *J. Mol. Catal.* **48**, 129 (1988).
- Saussine, L., Brazi, E., Robine, A., Mimoun, H., Fischer, J., and Weiss, R., *J. Am. Chem. Soc.* **107**, 3534 (1985).
- Groves, J. T., *Adv. Inorg. Biochem.* **1**, 119 (1979).
- White, R. E., and Coon, M. J., *Ann. Rev. Biochem.* **49**, 315 (1980).
- Guengerich, F. P., and MacDonald, T., *Acc. Chem. Res.* **17**, 9 (1984).
- Hamilton, G. A., in "Molecular Mechanisms of Oxygen Activation" (O. Hayaishi, Ed.), p. 405. Academic Press, New York, 1974.
- Ortiz de Montellano, P. R., in "Cytochrome P-450" (P. R. Ortiz de Montellano, Ed.), p. 235. Plenum, New York, 1986.
- McKenna, E. J., and Coon, M. J., *J. Biol. Chem.* **245**, 3882 (1970).
- Colby, J., and Dalton, H., *Biochem. J.* **157**, 495 (1976).
- Woodland, M. P., and Dalton, H. J., *J. Biol. Chem.* **259**, 53 (1984).
- Balch, A. L., Chen, Y. W., Cheng, R. J., LaMar, G. N., Latos-Grazynski, L., and Renner, M. W., *J. Am. Chem. Soc.* **106**, 7779 (1984).
- Reviewed in Momenteau, M., and Reed, C. A., *Chem. Rev.* **94**, 659 (1994).
- Ozawa, S., Watanabe, Y., Nakashima, S., Kitigawa, T., and Morishima, I., *J. Am. Chem. Soc.* **116**, 634 (1994).
- Paulson, D. R., Ullman, R., and Sloane, R. B., *J. Chem. Soc. Chem. Commun.*, 186 (1974).
- Dolphin, D., and Felton, R. H., *Acc. Chem. Res.* **7**, 26 (1973).
- Traylor, P. S., Dolphin, D., and Traylor, T. G., *J. Chem. Soc. Chem. Commun.*, 279 (1984).
- Chin, D., Balch, A. L., and LaMar, G. N., *J. Am. Chem. Soc.* **102**, 1446 (1980).
- Al-Malaika, D., "Atmospheric Oxidation and Antioxidants" (G. Scott, Ed.), p. 45. Elsevier, New York, 1993.
- Howard, J., "Free Radicals, Vol. II" (J. Kochi, Ed.), p. 3. Wiley, New York, (1970).

58. Howard, J., Chenier, J., and Holden, D., *Can. J. Chem.* **56**, 170 (1978).
59. Lyons, J. E., Ellis, P. E., Jr., Myers, H. K., and Wagner, R. W., *J. Catal.* **141**, 311 (1993).
60. Labinger, J. A., *Catal. Lett.* **26**, 95 (1994).
61. Kochi, J. K. (Ed.), "Free Radicals, Vol. II" p. 683. Wiley, New York, 1973.
62. Greene, F. D., Savitz, M. L., Osterholtz, F. D., Lau, H. H., Smith, W. N., and Zanet, P. M., *J. Org. Chem.* **28**, 55 (1963).
63. Summerville, D. A., Jones, R. D., Hoffman, B. M., and Basolo, F., *J. Am. Chem. Soc.* **99**, 8195 (1977).
64. Buchler, J. W., and Dreher, C., *Z. Naturforsch* **396**, 222 (1984).
65. Summerville, D. A., and Cohen, I. A., *J. Am. Chem. Soc.* **98**, 1747 (1976).
66. Ledon, H., *C. R. Acad. Sci. Paris* **288**, C29 (1979).
67. Donohoe, R. J., Atamian, M., and Bocian, D. F., *J. Am. Chem. Soc.* **109**, 5593 (1987).
68. Traylor, P. S., Dolphin, D., and Traylor, T. G., *J. Chem. Soc. Chem. Commun.*, 279 (1984).
69. Jayaraj, K., Gold, A., Toney, G. E., Helms, J. H., and Hatfield, W. E., *Inorg. Chem.* **25**, 3516 (1986).
70. Liston, D. J., and West, B. O., *Inorg. Chem.* **24**, 1568 (1985).
71. Banfi, S., Montanari, F., and Quici, S., *J. Org. Chem.* **53**, 2863 (1988).
72. Siegl, W. O., *J. Org. Chem.* **42**, 1872 (1977).
73. The apparent initial first-order rate constant for the Fe(TPPF₂₀β-Br₈)Cl-catalyzed oxidation of isobutane at 80°C ([catalyst] = 4.33 × 10⁻³ M; *i*-C₄H₁₀, 25 wt% in benzene; 100 psig O₂) was found to be: $k = 0.19 \text{ h}^{-1}$, whereas when Co(BPI)(O₂Bu⁺) was used under similar conditions, $k = 0.015 \text{ h}^{-1}$. The initial apparent first-order rate constant for the Fe(TPPF₂₀β-Cl₈)OH-catalyzed oxidation of isobutane at 60°C was found to be $k = 0.074 \text{ h}^{-1}$ whereas when Co(BPI)(N₃) was used no apparent reaction occurred at this temperature. Prior to our work the cobalt BPI complexes were among the most active liquid phase alkane oxidation complexes known (39, 40). It can be seen that iron perhaloporphyrin complexes are more than an order of magnitude more active than the BPI complexes (Bhinde, M. V., and Lyons, J. E., unpublished results).